Available online at www.sciencedirect.com
ScienceDirect
Ultrasonics Sonochemistry 14 (2007) 229–234
Ultrasonics SONOCHEMISTRY
www.elsevier.com/locate/ultsonch

Ultrasonic-assisted size-controllable synthesis of Bi_2Te_3 nanoflakes with electrogenerated chemiluminescence

Bo Zhou [a,b], Bo Liu [a], Li-Ping Jiang [a], Jun-Jie Zhu [a,*]

[a] Key Laboratory of Analytical Chemistry for Life Science, School of Chemistry and Chemical Engineering, Nanjing University, Nanjing 210093, PR China
[b] College of Chemistry and Environment Science, Nanjing Normal University, PR China

Received 12 December 2005; received in revised form 29 March 2006; accepted 5 April 2006
Available online 26 July 2006

Abstract

Bi_2Te_3 hexagonal nanoflakes with controllable edge length ranging from ~150 nm to as small as ~10 nm were synthesized via an ultrasonic-assisted disproportionation route, using Te powder and $Bi(NO_3)_3 \cdot 5H_2O$ as raw materials. The mechanochemical effects of the ultrasonic irradiation accelerated the reaction and were helpful to obtain relatively small and uniform nanocrystals. The products were characterized by X-ray powder diffraction, X-ray photoelectron spectra, transmission electron microscopy, and selected area electron diffraction techniques. Electrogenerated chemiluminescence of as-prepared Bi_2Te_3 was also reported for the first time.

Keywords: Thermoelectric materials; Bi_2Te_3 nanocrystals; Size-controllable; Ultrasonic; Disproportionation; Electrogenerated chemiluminescence

1. Introduction

The synthesis of nanostructured Bi_2Te_3 and its alloys has drawn more and more attention recently. On the one hand, the bismuth–telluride based alloys are known as the best thermoelectric materials currently available for thermoelectric application near room temperature [1,2]; on the other hand, theoretic [3,4] and experimental results [5,6] have shown that the quantum confinement effects in nanostructured materials can improve the efficiency of thermoelectric materials greatly.

As a parent compound to many important thermoelectric semiconductor alloys, bismuth–telluride (Bi_2Te_3) has been synthesized through different methods. Conventionally, it has been prepared through the metallurgical melt processing by mixing the appropriate amounts of the pure elements at elevated temperature of 500–600 °C [7,8]. Recently, some new synthetic routes were developed to synthesize Bi_2Te_3, such as the chemical [9] and mechanical alloying [10] methods, metal–organo complex method [11], solvothermal-reduction synthetic technique [12–14], reverse micelle process [15], and electrodeposition [16–18].

Because the efficiency of thermoelectric materials can be tailored by controlling the size and the shape of nanocrystals, the controllable synthesis of nanoscale thermoelectric materials is very important. Herein, we report a novel ultrasonic-assisted disproportionation method to synthesize Bi_2Te_3 hexagonal nanoflakes with controllable size ranging from ~150 nm to as small as ~10 nm. This size controllability and the smallness of the size of the products make this method very interesting.

Sonochemical methods have been extensively explored to synthesize various nanostructured materials, such as metal colloids, semiconductor powders and nanorods [19–25]. During sonication, microscopic bubbles form and grow in the low pressure stage, and subsequently collapse in the high pressure stage [23,24], causing hot spots-localized regions of extremely high temperatures as high as 5000 K, and pressures of up to ~1800 atm, and cooling rates can often exceed $\sim 10^{10}$ K s^{-1}[19]. These extreme conditions have been exploited to prepare nanoscale materials. Mechanochemical effects of the ultrasonic irradiation also

* Corresponding author. Tel.: +86 25 83594976; fax: +86 25 83317761.
E-mail address: jjzhu@nju.edu.cn (J.-J. Zhu).

1350-4177/$ - see front matter © 2006 Published by Elsevier B.V.
doi:10.1016/j.ultsonch.2006.04.001

play important roles, especially in the heterogeneous systems [26,27].

Though the Bi_2Te_3 based materials are known as the best thermoelectric materials near room temperature, in this work, we found, for the first time, the electrogenerated chemiluminescence of as-prepared Bi_2Te_3 nanoflakes.

2. Experimental

All reagents were commercially available (Te, from Acros Organics; $Bi(NO_3)_3 \cdot 5H_2O$, from Peking Chemical Reagent Institution; KOH, from Shanghai Chemical Reagent Co., LTD; EG, from Shanghai Tingxin Chemical Reagent Factory) and used without further purification.

In a typical procedure, bismuth nitrate ($Bi(NO_3)_3 \cdot 5H_2O$, 2/3 mmol), potassium hydroxide (KOH, 0.5–4 g), and elemental telluride powder (Te, 1 mmol) were added into 30 ml of solvent, which can be the mixture of glycerol and water, ethylene glycol (EG), or EG containing certain amount of polyvinyl pyrrolidone (PVP, K-30). Then the mixture was sonicated for 5 h by putting an ultrasonic probe into it. The temperature of the reaction system increased to ~95 °C in 10 min, reached ~120 °C in 30 min, and remained at ~122 °C after 40 min. The black precipitate obtained was centrifuged, washed with distilled water and absolute ethanol subsequently, and dried under vacuum at room temperature.

Sonication was performed using a VCX 750 Vibra-Cell high intensity ultrasonic processor (Sonics & Materials, USA) equipped with an immersion ultrasonic probe, which was made of titanium alloy TI-6AL-4V, and with the tip diameter of 13 mm. The frequency is 20 kHz, and the net power output is 750 W. The variable power output control allows the ultrasonic vibrations at the probe tip to be set to any desired amplitude. With the amplitude control set at 100%, the amplitude at the tip with diameter of 13 mm is 124 μm. In our work, the amplitude control was set at 35%. The pulse cycle of 9 s on and 1 s off was set via the independent on/off pulser.

The X-ray diffraction (XRD) patterns of the products were recorded with a Philips X'pert X-ray diffractometer (using Cu-Kα radiation, $\lambda = 1.5418$ Å). The X-ray photoelectron spectra (XPS) of the products was recorded on ESCALAB MK II X-ray photoelectron spectrometer, using non-monochromatized Mg-Kα radiation as the excitation source and choosing C1s (284.6 eV) as the reference line. The transmission electron microscope (TEM) images and selected area electron diffraction (SAED) patterns were obtained using a JEM-200CX (JEOL, 200 kV) TEM.

Electrogenerated chemiluminescence measurements were carried out in 0.05 M $K_2S_2O_8$ + 0.1 M KOH aqueous solution containing 0.1 M KCl on a Model MPI-A Electrochemiluminescence Analyzer Systems (Xi'an Remax Electronic Science & Technology Co. Ltd., Xi'an, China). A three-electrode system was employed with Pt wire as a counter electrode, Ag/AgCl as a reference electrode, and a carbon-paste electrode as a working electrode. The carbon-paste electrode was fabricated as follows: graphite powder and as-prepared Bi_2Te_3 nanoflakes were thoroughly mixed with a weight ratio of 3:1 in ethanol solvent by ultrasonic dispersion. After drying under stirring, a homogenized graphite/Bi_2Te_3 mixture was achieved. Subsequently, paraffin oil was added to the mixture and mixed fully until a homogeneous paste was obtained. The prepared paste was packed into a glass tube with a 4 mm inner diameter and electrical contact was established with a copper rod through the back of the homemade electrode. The electrode surface was polished with smoothing paper.

3. Results and discussion

XRD measurements were carried out to determine the crystalline phase of as-prepared products. The typical XRD pattern of the products is shown in Fig. 1. All the diffraction peaks can be indexed to the hexagonal structure phase for Bi_2Te_3 (JCPDS Files No. 15-0863). No peaks of any other phases are detected, indicating the high purity of the products. And no unreacted Te was detected in the products, indicating the reaction was complete.

The X-ray photoelectron spectra (XPS) are shown in Fig. 2. The peaks at energies of ~157.5 and ~162.5 eV, which are pointed at by arrows in Fig. 2b, correspond to the binding energy of Bi 4f7/2 and Bi 4f5/2 of Bi_2Te_3. The peaks at energies of 571.9 and 582.3 eV, which are shown in Fig. 2c, correspond to the binding energy of Te 3d5/2 and Te 3d3/2 of Bi_2Te_3. These results are in good agreement with that observed from Bi_2Te_3 single crystal. The other peaks at energies of 158.8, 164.0, 575.6, and 586.0 eV shown in Fig. 2b and c, are in good agreement with the Bi 4f and Te 3d spectra of an oxidized layer of Bi_2Te_3 [28]. Quantification of the relevant XPS peaks gave an atomic ratio of 1:1.607 for Bi:Te, which is close to the value for the stoichiometric compound. These results lead

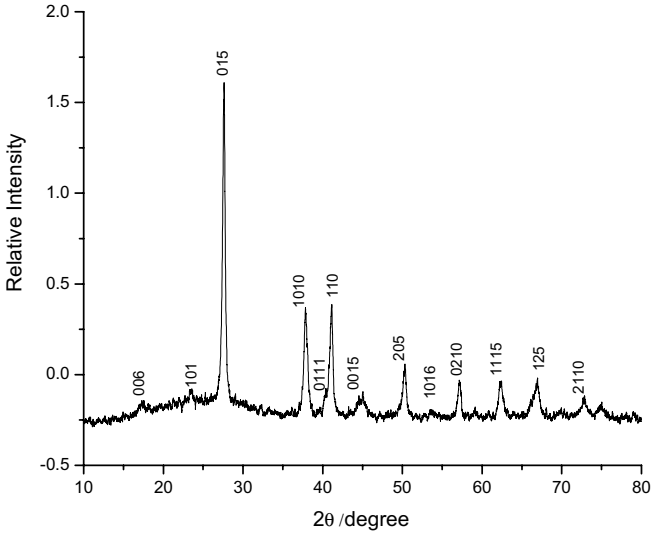

Fig. 1. The typical XRD pattern of as-prepared Bi_2Te_3 nanoflakes.

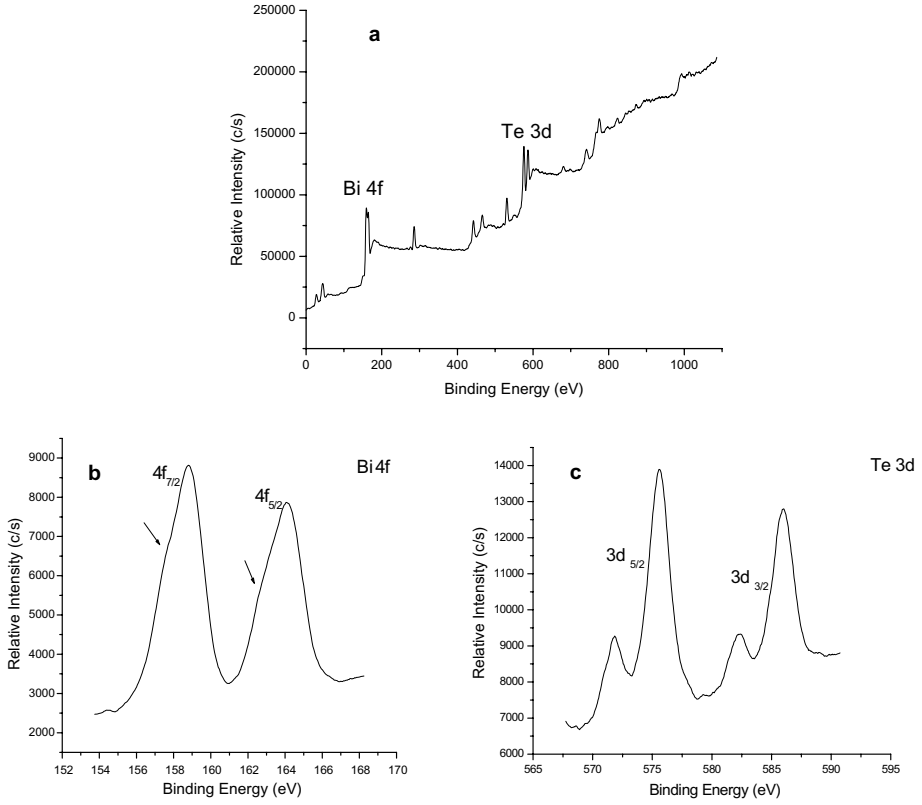

Fig. 2. The XPS spectra of as-prepared Bi_2Te_3 nanoflakes.

to a conclusion that the products obtained are Bi_2Te_3 particles with oxidized outside layers.

The morphology and the size of the produced particles can be observed in TEM images shown in Fig. 3. Fig. 3A–D show that as-prepared Bi_2Te_3 particles are hexagonal nanoflakes. This hexagonal flake-like morphology is a common morphology of the layered Bi_2Te_3 as reported in the Refs. [11b,29]. And this flake-like morphology was also confirmed by the TEM image shown in Fig. 5, where both flakes that parallel to and that perpendicular to the panel were shown. The nanoflakes with different size ranging from ~150 nm to as small as ~10 nm can be obtained in different conditions. The effects on the size of the Bi_2Te_3 particles will be discussed in the later part of this paper. Fig. 3E and F show the typical SAED patterns of an individual nanoflake and a set of nanoflakes, respectively, indicating the single-crystallinity of individual nanoflakes and the well crystallinity of the products. The SAED patterns also confirmed that the products were hexagonal Bi_2Te_3.

In this sonochemical synthesis of Bi_2Te_3, the disproportionation of Te in alkaline solution (Eq. (1)) played a crucial role. Te^{2-} produced in the disproportionation of Te reacted with Bi(III) to give out Bi_2Te_3 (Eq. (2)). The mechanism may be as follows:

$$3Te + 6OH^- \rightarrow 2Te^{2-} + TeO_3^{2-} + 3H_2O \quad (1)$$

$$2Bi^{3+} + 3Te^{2-} \rightarrow Bi_2Te_3 \quad (2)$$

The above mechanism is consistent with the following experimental facts: (A) The disproportionation of Te in condensed alkaline solution can be carried out to give out purple solution of Te^{2-}, as reported in the Ref. [30]. (B) No Bi^0 was detected by XRD during the reaction, and no solid Bi produced when the reaction was carried out in the absence of Te. This implied that the Bi_2Te_3 was not produced through the reaction of Bi with Te. (C) The alkali could accelerate the reaction. It is observed that the reaction speed increased along with the increment of KOH, because more KOH could drive Eq. (1) to move to the right side.

Sonication was an important factor in this synthesis of Bi_2Te_3 nanoflakes. Firstly, sonication accelerated the reaction. When the reaction was performed under stirring for 5 h in an oil bath of temperature of ~140 °C, which is higher than the temperature of the sonication system, large quantity of unreacted tellurium remained in the product, as evidenced by the XRD analysis shown in Fig. 4. Secondly, sonication was helpful to obtain relatively small and uniform particles. When the reaction was performed under solvothermal conditions (160 °C, 20 h), larger flakes with edges longer than 200 nm and aligned flakes [11b] were obtained (Fig. 5). The cavitation in liquid–solid systems produces mechanochemical effects, in addition to the homogeneous cavitation observed in pure liquids. Liquid jets and/or shock waves formed under ultrasound irradiation can cause surface damage of the solid and/or produce high velocity interparticle collisions [26,27,31]. These

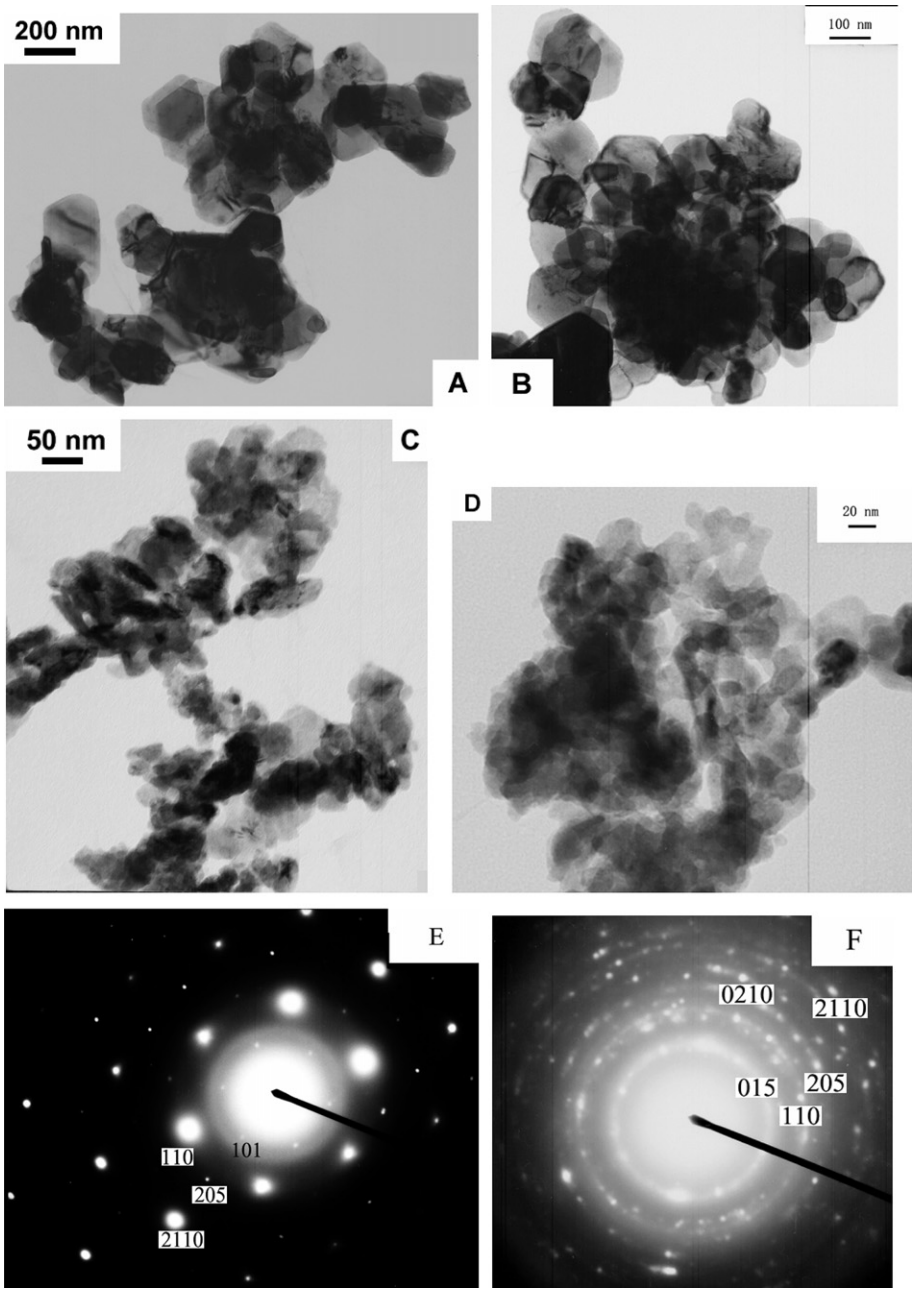

Fig. 3. (A–D): The TEM images of as-prepared Bi_2Te_3 nanoflakes obtained: (A) in the mixed solvent of glycerol and water with the volume ratio of 4/1; (B) in EG solvent; (C) when 0.05 g PVP was added into EG; (D) when 2 g PVP was added into EG. (E–F): The SAED patterns of an individual nanoflake and a set of nanoflakes (sample D), respectively.

effects, firstly, can produce particle breakage of Te, thus favored its dissolution and accelerated the reaction, and secondly, can prevent the aggregation of the resulting nanocrystals [32]. In addition, cavitation greatly accelerates mass transport [33], and makes the repassivation by reaction products less important or even avoidable [34]. This also accelerates the reaction.

The size of the Bi_2Te_3 nanoflakes changed when using different solvents. Fig. 3A shows the Bi_2Te_3 nanoflakes with edge length of ~150 nm, which were obtained when the mixture of glycerol and water with the volume ratio of 4/1 (when this ratio increased, too much glycerol made the solvent more viscid and harder to process; and when this ratio decreased, too much water slowed down the reaction.) was used as solvent. And when the solvent changed to EG, the size of the nanoflakes obtained changed to $80 \sim 100$ nm, as shown in Fig. 3B.

Addition of a certain amount of PVP can also affect the size of the Bi_2Te_3 nanocrystals. When 0.05 g PVP was added into EG, the size of the nanoflakes decreased from $80 \sim 100$ nm to $40 \sim 50$ nm, as shown in Fig. 3C. When the quantity of the PVP added increased to 0.5 g, the size of the nanoflakes decreased to ~10 nm. The reason might be that the PVP added into EG could adsorb onto the sur-

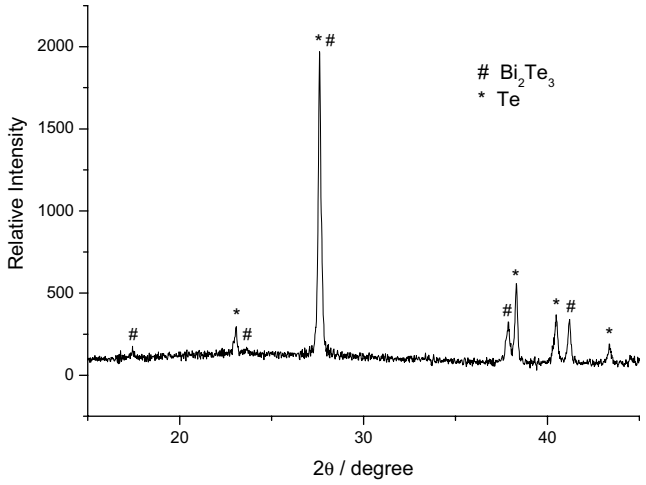

Fig. 4. The XRD pattern of the products obtained under stirring for 5 h in an oil bath of temperature of ~140 °C.

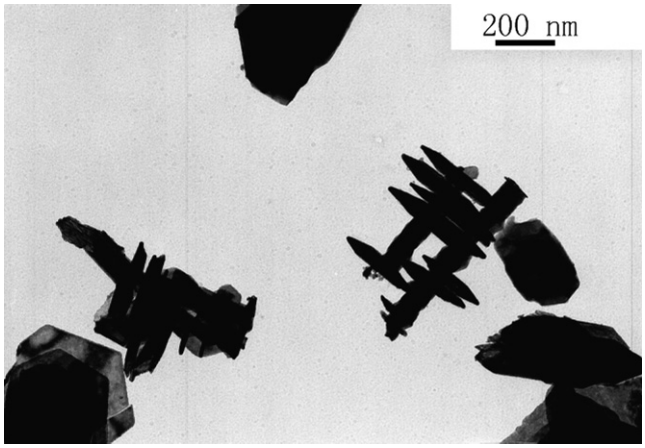

Fig. 5. The TEM image of Bi_2Te_3 nanoflakes obtained under solvothermal conditions (160 °C, 20 h).

faces of the nanoflakes and hinder their growth, resulting in the formation of nanoflakes with smaller size. However, 10 nm seemed to be the limit of the size of as-prepared Bi_2Te_3 nanoflakes. Even when the quantity of PVP in the reaction system increased to 2 g, the size of the nanoflakes were still ~10 nm (Fig. 3D), and did not decrease further obviously. This might attribute to that when the nanoflake surfaces were occupied completely, the excess PVP would remain free (unadsorbed to the nanoflakes) in the solution, and the decrease of the size reached its limit.

The ECL behavior of the Bi_2Te_3 nanoflakes at a carbon-paste electrode in aqueous solution was studied under conventional cyclic voltammetry (CV). Fig. 6 shows the typical ECL emission of Bi_2Te_3 nanoflakes under continuous potential scanning for six cycles. The electrode potential was cycled between 0.1 V and −1.5 V at a scan rate of 125 mV s^{-1}. ECL is generated by relaxation of excited-state molecules that are produced through electron-transfer annihilation of electrogenerated anion and cation radicals [35]. In the case of the ECL of Bi_2Te_3, the mechanism might be as follows: as the electrode potential is made more

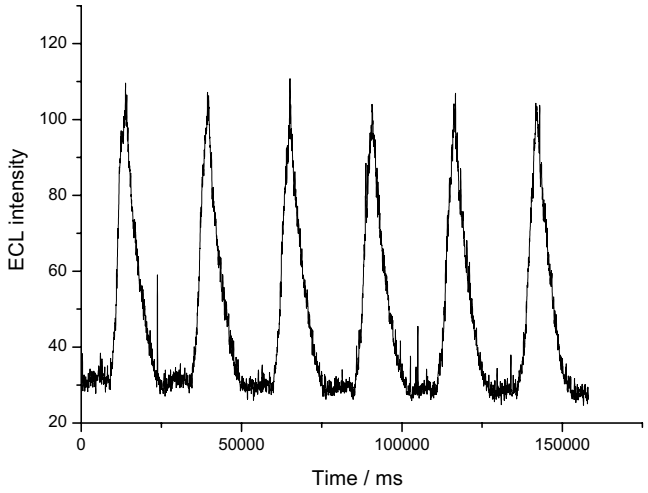

Fig. 6. ECL emission from Bi_2Te_3 nanoflakes in 0.05 M $K_2S_2O_8$ + 0.1 M KOH aqueous solution containing 0.1 M KCl under continuous cyclic voltammetry for six cycles.

negative, electrons are injected into the Bi_2Te_3 nanoflakes and electrogenerated anion radicals ($Bi_2Te_3^{-\cdot}$) are formed. Concurrently, $S_2O_8^{2-}$ ions were added as a co-reactant to produce a strong oxidant, $SO_4^{-\cdot}$ [35,36]. The formed sulfate radicals can react with the negatively charged Bi_2Te_3 nanoflakes to produce excited states and then generate light emission. The supporting evidence is that in the experiment, the ECL is not obvious in the absence of $S_2O_8^{2-}$. This result implied that Bi_2Te_3 might be used as an electrogenerated chemiluminescent material.

$$S_2O_8^{2-} + e^- \rightarrow SO_4^{2-} + SO_4^{-\cdot} \quad (3)$$

$$Bi_2Te_3^{-\cdot} + SO_4^{-\cdot} \rightarrow Bi_2Te_3^{*} + SO_4^{2-} \quad (4)$$

4. Conclusions

Bi_2Te_3 hexagonal nanoflakes with controllable size varying from ~150 nm to as small as ~10 nm were synthesized via an ultrasonic-assisted disproportionation route. It was found that sonication played an important role in the formation of small and uniform Bi_2Te_3 nanoflakes. The size of the nanoflakes also depended on the different solvents and various amount of PVP added. The size controllability makes this method promising to synthesis thermoelectric materials with controllable performance. What is more, considering that the Te^{2-} would react with other cations supplied, we think this disproportionation route should be a general route to synthesize other tellurides, such as Sb_2Te_3, ZnTe, etc. Electrogenerated chemiluminescence of Bi_2Te_3 was also reported, for the first time.

Acknowledgements

This work is supported by the National Natural Science Foundation of China (Grant Nos. 20325516 and 9020603), and "863" Project (No. 2003AA302740). This work is also

supported by the National Natural Science Foundation of China for Creative Research Groups (20521503).

References

[1] A. Boyer, E. Cisse, Mater. Sci. Eng. B 113 (1992) 103.
[2] F.J. DiSalvo, Science 285 (1999) 703.
[3] L.D. Hicks, M.S. Dresselhaus, Phys. Rev. B 47 (1993) 12727.
[4] L.D. Hicks, M.S. Dresselhaus, Phys. Rev. B 47 (1993) 16631.
[5] S.H. Yu, M. Yoshimura, Adv. Mater. 14 (2002) 296.
[6] R. Venkatasubramanian, E. Siivola, T. Colpitts, B. O'Quinn, et al., Nature 413 (2001) 597.
[7] C. Kaito, Y. Saito, K. Fujita, J. Cryst. Growth 94 (1989) 967.
[8] F.D. Rosi, B. Ables, R.V. Jensen, J. Phys. Chem. Solids 10 (1959) 191.
[9] M. Toprak, Y. Zhang, M. Muhammed, Mater. Lett. 57 (2003) 3976–3982.
[10] S. Hu, X. Zhao, T. Zhu, Rare Metal Mater. Eng. 31 (4) (2002) 287–290.
[11] (a) J.J. Ritter, P. Maruthamuthu, Inorg. Chem. 34 (1995) 4278;
(b) W.G. Lu, Y. Ding, Y.X. Chen, Z.L. Wang, J.Y. Fang, J. Am. Chem. Soc. 127 (2005) 10112–10116.
[12] Y. Deng, C. Nan, G. Wei, L. Guo, Y. Lin, Chem. Phys. Lett. 374 (3–4) (2003) 410–415.
[13] C. Wang, K. Tang, Q. Yang, J. Hu, Y. Qian, J. Mater. Chem. 12 (8) (2002) 2426–2429.
[14] S. Yu, J. Yang, Y. Wu, Z. Han, J. Lu, Y. Xie, Y. Qian, J. Mater. Chem. 8 (9) (1998) 1949–1951.
[15] E.E. Foos, R.M. Stroud, A.D. Berry, Nano. Lett. 1 (2001) 693.
[16] M.M. Gonzalez, G. Snyder, A. Prieto, R. Gronsky, T. Sands, A. Stacy, Nano Lett. 3 (7) (2003) 973–977.
[17] M.M. Gonzalez, A. Prieto, M. Knox, R. Gronsky, T. Sands, A. Stacy, Chem. Mater. 15 (8) (2003) 1676–1681.
[18] M. Sander, A. Prieto, R. Gronsky, T. Sands, A. Stacy, Adv. Mater. 14 (9) (2002) 665–667.
[19] K.S. Suslick, Science 247 (1990) 1439.
[20] C.L. Bianchi, R. Carli, S. Lanzani, D. Lorenzetti, G. Vergani, V. Ragaini, Ultrason. Sonochem. 1 (1994) S47.
[21] (a) Y. Koltypin, G. Katabi, R. Prozorov, A. Gedanken, J. Non-cryst. Solids 201 (1996) 159;
(b) J.J. Zhu, Y. Koltypin, A. Gedanken, Chem. Mater. 12 (2000) 73.
[22] S.V. Ley, C.M.R. Low, Ultrasound in Synthesis, Springer-Verlag, New York, 1989.
[23] T.J. Mason, J.P. Lorimer, Sonochemistry: Theory, Applications and Uses of Ultrasound in Chemistry, John Wiley and Sons, New York, 1988.
[24] K.S. Suslick, Ultrasound: Its Chemistry, Physical, and Biological Effects, VCH Publishers., New York, 1988.
[25] H. Wang, J.J. Zhu, J.M. Zhu, H.Y. Chen, J. Phys. Chem. B 106 (2002) 3848.
[26] P. Jeevanandam, Y. Diamant, M. Motiei, A. Gedanken, Phys. Chem. Chem. Phys. 3 (2001) 4107–4112.
[27] Pedro Cintas, Jean-Louis Luche, Green Chem. 1 (3) (1999) 115.
[28] H. Bando, K. Koizumi, Y. Oikawa, et al., J. Phys: Condens. Mater. 12 (2000) 5607.
[29] D. Wang, D. Yu, M. Mo, X. Liu, Y. Qian, J. Cryst. Growth 253 (2003) 445–451.
[30] (a) G. Kirschstein, G. Czack, D. Koschel, H.K. Kugler (Eds.), Gmelin Handbook of Inorganic Chemistry, eight ed., Tellurium Supplement, vol. 2A, Springer-Verlag, Berlin, Heindelberg, 1983, p. 386;
(b) Bo Zhou, Jian-Rong Zhang, Liang Zhao, Jian-Min Zhu, Jun-Jie Zhu, Ultrason. Sonochem 13 (2006) 352–358.
[31] Aharon Gedanken, Ultrason. Sonochem. 11 (2004) 47–55.
[32] Q. Li, Y. Ding, M.W. Shao, J. Wu, G.H. Yu, Y.T. Qian, Mater. Res. Bull. 38 (2003) 539–543.
[33] L.C. Hagenson, L.K. Doraiswamy, Chem. Eng. Sci. 53 (1997) 131.
[34] (a) A. Benhacene, P. Labbé, C. Petrier, G. Reverdy, New J. Chem. 19 (1995) 989;
(b) J. Klima, C. Bernard, C. Degrand, J. Electroanal. Chem. 367 (1994) 297.
[35] Z. Ding, B.M. Quinn, S.K. Haram, L.E. Pell, B.A. Korgel, A.J. Bard, Science 296 (2002) 1293–1297.
[36] S.K. Poznyak, D.V. Talapin, E.V. Shevchenko, H. Weller, Nano Lett. 4 (4) (2003) 693–698.